Is NO_3 Formed during the Decomposition of Nitramine Explosives?

Karl K. Irikura* and Russell D. Johnson, III

Computational Chemistry Group, National Institute of Standards and Technology, Gaithersburg, Maryland 20899-8380

Received: August 29, 2006; In Final Form: November 1, 2006

Quantum chemistry calculations reveal that it is both thermodynamically and kinetically feasible for NO_2 to be oxidized by RDX (1,3,5-trinitrohexahydro-*s*-triazine) or its initial decomposition products. Thus, NO_3 (nitrate radical) may be produced during the thermal decomposition of RDX and other nitramines. However, experimental studies of the gaseous products, by mass spectrometry and microwave spectroscopy, have never detected NO_3. This fact is reconciled with the calculations by noting that (1) the electron-impact, positive-ion mass spectrum of NO_3 shows little parent ion, (2) NO_3 lacks a permanent electric dipole moment and is therefore invisible to microwave spectroscopy, and (3) NO_3 is quite reactive. Further experiments are encouraged and could lead to a new method for detecting concealed nitramines.

Introduction

RDX, also commonly known as hexogen, cyclonite, or 1,3,5-trinitrohexahydro-*s*-triazine (structure shown in Scheme 1) is the most widely used high explosive and is an important high-energy propellant. Although much has been learned from decades of experimental and theoretical studies, the detailed chemical mechanism of RDX decomposition is complex and only partly known. Much of the difficulty stems from the interplay between condensed-phase and gas-phase processes, which causes the product distribution to be sensitive to experimental conditions such as heating rate, pressure, temperature, and confinement. In addition, experimental investigations of the primary reaction products are hindered by the great speed of subsequent reactions. Usually it is only the final reaction products that are identified clearly.

Many reactions have been suggested as the initial step(s) in the decomposition of RDX.[1] Reactions 1−4 are some of the popular candidates. Product structures and labels are shown in Scheme 1, and reaction enthalpies and barriers are listed in Table 1. The papers cited in Table 1 are those that we believe to be the earliest published proposals for the corresponding reactions. The enthalpy changes and barrier heights in Table 1 are from published[2,3] calculations done using the popular B3LYP/6-31G(d) density-functional method.

$$\mathrm{RDX} \rightarrow \mathrm{RDR} + \mathrm{NO_2} \quad (1)$$

$$\mathrm{RDX} \rightarrow \mathbf{1} \quad (2)$$

$$\mathrm{RDX} \rightarrow 3\mathrm{H_2C{=}N{-}NO_2} \quad (3)$$

$$\mathrm{RDX} \rightarrow \mathbf{5} + \mathrm{HONO} \quad (4)$$

We have investigated the early reactions of RDX decomposition using conventional methods of quantum chemistry, which are increasingly powerful and economical. New reactions were generated either by hand or by using isopotential searching (IPS) methods[4] on a semiempirical (PM3[5]) potential energy surface. Although this work was initiated merely to investigate the utility of IPS, the chemistry of nitramines has continued to hold our interest. In particular, studying unimolecular chemistry has led to the realization that bimolecular reactions are important in nitramine decomposition.

SCHEME 1

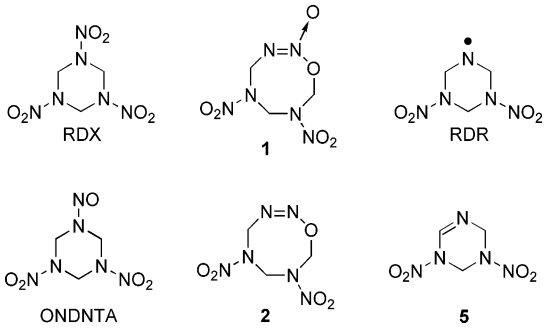

TABLE 1: Reaction Enthalpies and Barriers for Proposed Initiation Reactions[a]

reaction	ΔH_0 (kJ mol^{-1})	$\Delta H_0^{\ddagger}$ (kJ mol^{-1})	ref
1	+163	163	33
2	+59	220	34
3	+192	249	28, 35
4	−36	164	36

[a] B3LYP/6-31G(d) energies are by Chakraborty et al.[2,3] and are relative to RDX.

Although there have been many ab initio calculations of nitramine chemistry, bimolecular reactions have received little theoretical attention since the pioneering work by Melius and co-workers.[6] Experimentally, bimolecular chemistry has been addressed, for example, by the isotope crossover experiments done by Behrens and Bulusu.[7] In those experiments, a mixture of two isotopologues was thermolyzed and the products were analyzed by mass spectrometry. Although initial steps cannot be inferred from the end products alone, isotopic studies provide constraints. For example, both nitrogen atoms in product N_2O come from the same molecule of RDX (i.e., no crossover), whereas the nitroso derivative of RDX ("ONDNTA", see Scheme 1) shows both nitrogen and hydrogen crossover.

10.1021/jp065611d
Published on Web 12/21/2006

Computational Methods

Qualitative unimolecular reactions of RDX were sought by using isopotential searching on a PM3 potential energy surface, denoted IPS//PM3. Such computations require on the order of hours on a laptop personal computer. IPS performs best for reactions with loose transition states; tight transition states occupy only small volumes in coordinate space and consequently are less probably encountered during a search. The Gaussian 98,[8,9] GAMESS,[10,11] and PC-GAMESS[12] software packages were used at various times for the PM3 calculations. PM3 was used for its efficiency; ab initio IPS is tediously slow. Interesting results from the IPS//PM3 investigations were always verified (or refuted) by using more reliable calculations.

IPS trajectories were analyzed both visually and by using an automated procedure that produces preliminary minimum-energy and saddle-point structures. Subsequently, quantitative gas-phase energies were computed using density functional theory (DFT) with the hybrid functional B3LYP[13−15] and the 6-31G(d) basis sets (Cartesian polarization functions, "6D"). The Gaussian 98[9] and Gaussian 03[16] program packages were used for the DFT calculations, but all reported quantities were obtained using Gaussian 03 for consistency. All structures were fully optimized and characterized by vibrational analysis as either energy minima or first-order saddle points. The reactant(s) and product(s) corresponding to each transition structure were verified by intrinsic reaction coordinate (IRC[17]) calculations. Vibrational zero-point energies (ZPEs) were computed as one-half the sum of the harmonic frequencies and then multiplied by 0.9806 as recommended.[18] Thermodynamic functions were computed by using the rigid rotor/harmonic oscillator approximation and unscaled frequencies. There are some very low vibrational frequencies, which are probably anharmonic. The entropy and heat capacity are underestimated in such cases. The atomic unit of energy, the hartree, is $E_h \approx 2625.5$ kJ/mol. The symbol E_e denotes an electronic energy that does not include ZPE. The symbol E_0 denotes an electronic energy to which ZPE has been added. All energy differences reported here include ZPE.

To estimate the uncertainty of our computed reaction enthalpies, we examine the performance of B3LYP/6-31G(d) for computing atomization enthalpies. There are data (at 298 K) for 39 CHNO molecules in the Computational Chemistry Comparison and Benchmark Database.[19] The mean value of E_{dif} (difference between theoretical and experimental values) is $\langle E_{dif} \rangle = -24.1$ kJ/mol, which represents the bias in the calculated atomization enthalpies. We assume that this bias will be similar for the reactants and products of a typical reaction, so that it cancels out of the reaction enthalpy. The standard uncertainty for the reaction enthalpy may then be estimated as the standard deviation, σ_{dif}, of E_{dif} about its mean. This may be evaluated as $\sigma_{dif}^2 = \langle E_{dif}^2 \rangle - \langle E_{dif} \rangle^2$, where the rms (root-mean-square) difference is $\langle E_{dif}^2 \rangle^{1/2} = 32.5$ kJ/mol. The result, $\sigma_{dif} = 22$ kJ/mol, is the estimated standard uncertainty for *any* B3LYP/6-31G(d) reaction enthalpy involving molecules composed only of the elements C, H, N, and O (at least one atom of each). This precision is adequate for the present semiquantitative purposes, but it is clearly inadequate for the computation of reaction rates. Restricting the analysis to nitramines and related molecules would probably lead to smaller estimated uncertainties because it is a narrower classification,[20] but the appropriate definition of "related molecules" is itself uncertain.

Results

As in earlier work by others,[21] we found the lowest-energy ($E_e = -897.409363$ E_h) conformation of RDX to be one of C_s symmetry, with two nitro groups axial (*cis*) and one equatorial. However, the all-axial conformation ($E_e = -897.408898$ E_h), of C_{3v} symmetry, is only 0.6 kJ/mol less stable (all conformational energy differences are at zero temperature, that is, ΔE_0). A conformation with one equatorial and two *trans*-axial nitro groups ($E_e = -897.408338$ E_h) is 3.1 kJ/mol less stable than the lowest-energy conformation. Since our calculations are approximate, such small energy differences may not be meaningful.

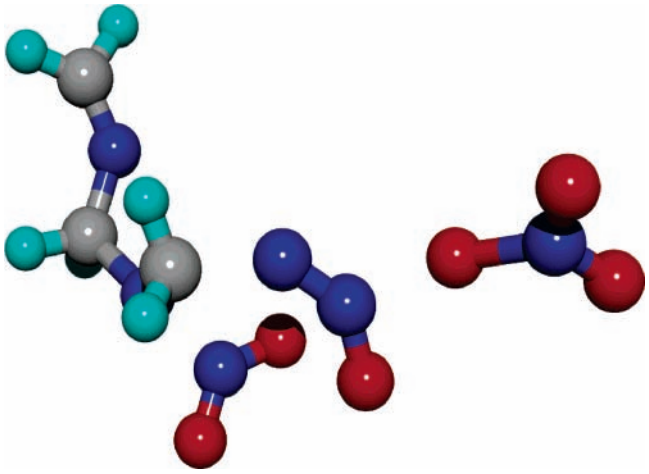

Figure 1. Snapshot from IPS//PM3 investigation of unimolecular decomposition of RDX showing NO_3 formation.

For reduced RDX (ONDNTA in Behrens' nomenclature[7]), we also found three stable conformations. The most stable ($E_e = -822.227187$ E_h) has one nitro group (on the oxo side of the bent nitroso group) equatorial and the other axial. The all-axial conformation ($E_e = -822.226989$ E_h) and the other axial−equatorial conformation ($E_e = -822.226389$ E_h) are less stable by 0.4 and 1.9 kJ/mol, respectively.

For compound **1** we identified three conformational isomers. The most stable has one nitro group equatorial and the other axial ($E_e = -897.386090$ E_h). A *trans*-axial conformation ($E_e = -897.383013$ E_h) and an all-equatorial conformation ($E_e = -897.379571$ E_h) are 7.4 and 16.2 kJ/mol less stable, respectively.

We also found three stable conformations for compound **2** (reduced **1**). The most stable ($E_e = -822.212352$ E_h) is *trans*-axial, followed by axial (near the ring oxygen)−equatorial ($E_e = -822.210869$ E_h) and equatorial−axial ($E_e = -822.205394$ E_h), which are 4.3 and 18.0 kJ/mol less stable, respectively.

IPS calculations repeatedly suggested many unimolecular reactions of RDX, including reactions 1 and 2. Additional reactions, including reaction 4, were produced by the automated analysis of the IPS trajectories. Some novel reactions, when further investigated using DFT, were judged energetically unreasonable. As a marginal example, Figure 1 shows a representative frame from one reaction that "occurred" several times. NO_3 departed after ring-opening, as shown in Scheme 2. Calculated energies, entropies, and enthalpy contents (i.e., integrated heat capacities C_v) are listed in Table 2. The ring-opening reaction of RDX to form intermediate **3** is endothermic, with $\Delta H_0 = 143$ kJ/mol and $\Delta G_{298} = 133$ kJ/mol (see Table 3). Thus, this reaction is thermodynamically comparable to those listed in Table 1. However, the barrier is high, $\Delta H_0^{\ddagger} \simeq 247$ kJ/mol, suggesting that this process is not competitive with reactions 1 and 4.

Although the reaction sequence of Scheme 2 may be unimportant at low temperatures, it suggested the possibility

SCHEME 2

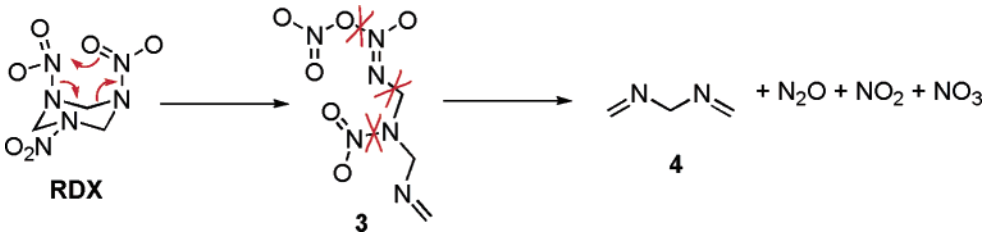

TABLE 2: Molecular and Transition-Structure Energies (B3LYP/6-31G*, including scaled ZPE) at 0 K, Gas-Phase Standard Entropies at 298 K, and Gas-Phase Enthalpy Contents at 298 K

molecule	E_0 (hartree)	$S°_{298}$ (J mol^{-1} K^{-1})	$H_{298} - H_0$ (kJ/mol)
RDX	−897.268612	478.1	35.4
ONDNTA	−822.091907	462.0	33.7
1	−897.245877	472.9	35.3
2	−822.077692	451.4	33.4
3	−897.214008	531.8	40.5
4	−227.280464	308.7	17.3
N_2O	−184.649270	219.8	9.5
NO_2	−205.063553	240.2	10.2
NO_3	−280.206435	266.4	13.2
NO	−129.883708	211.2	8.7
N_2	−109.518641	191.7	8.7
$ONONO_2$	−410.130338	331.1	18.0
N_2O_4	−410.145216	301.6	16.4
H_2NNO_2	−260.992651	268.2	12.1
H_2NNO	−185.811734	255.5	12.1
TS(RDX → **3**)	−897.174674	470.6	36.4
^{3}TS($2NO_2$ → NO + NO_3)	−410.055234	334.6	17.6
TS(N_2O + NO_2 → N_2 + NO_3)	−389.645459	330.9	17.4
TS(H_2NNO_2 + NO_2 → H_2NNO + NO_3)	−466.004282	348.8	19.9
TS(RDX + NO_2 → ONDNTA + NO_3)	−1102.280508	539.4	42.8
TS(**1** + NO_2 → **2** + NO_3)	−1102.256497	554.8	43.4

that NO_3 might be formed in a bimolecular reaction, by oxygen-atom abstraction. That is, sometimes NO_2 might act as a reducing agent. NO_2 is expected to be abundant because it is a product of the widely accepted initiation step involving homolytic N−N cleavage, reaction 1. Potential reaction partners include other early products and RDX itself. A few plausible bimolecular reactions of NO_2 are shown below, along with thermochemistry computed from the data in Table 2.

$$\text{RDX} + \text{NO}_2 \rightarrow \text{ONDNTA} + \text{NO}_3 \quad \Delta H_0 = 89 \text{ kJ/mol} \quad (5)$$

$$\text{NO}_2 + \text{NO}_2 \rightarrow \text{NO} + \text{NO}_3 \quad \Delta H_0 = 97 \text{ kJ/mol} \quad (6)$$

$$\mathbf{1} + \text{NO}_2 \rightarrow \mathbf{2} + \text{NO}_3 \quad \Delta H_0 = 66 \text{ kJ/mol} \quad (7)$$

All three of these reactions have thermodynamic energy requirements smaller than the barriers for initiation listed in Table 1. However, barrier heights are required to evaluate the feasibility of these reactions at low temperatures.

Since computing converged transition structures can be challenging, it is often expeditious to begin with a smaller but related system. As an analogue for reaction 5, we first computed a transition structure for the model reaction H_2NNO_2 + NO_2 → H_2NNO + NO_3. This yielded ΔH_0 = 100 kJ/mol and the barrier $\Delta H_0^{\ddagger}$ = 136 kJ/ mol. The important geometric parameters from this structure were used as the starting point in searches

TABLE 3: Ideal-Gas Reaction Energetics Based upon Data in Table 2

reaction	ΔH_0 (kJ mol^{1-})	ΔS_{298} (J mol^{-1} K^{-1})	ΔG_{298} (kJ mol^{-1})	$\Delta H_0^{\ddagger}$ (kJ mol^{-1})
RDX → **3**	143	54	133	247
RDX + NO_2 → ONDNTA + NO_3	89	10	87	136
3 → **4** + N_2O + NO_2 + NO_3	38	503	−103	*a*
$2NO_2$ → NO + NO_3 (triplet)	97	−3	99	189
$2NO_2$ → $ONONO_2$	−8	−149	34	0
$ONONO_2$ → NO + NO_3	106	146	66	106
1 + NO_2 → **2** + NO_3	66	5	66	139

[a] Not computed.

for transition structures for oxygen-atom abstraction from the nitro groups of RDX, reaction 5. Three sites of attack were considered: at the equatorial nitro group (eq), at an axial nitro group and near the symmetry plane (aa), and at an axial nitro group near the equatorial nitro group (ae). Both *endo* (above the center of the RDX ring) and *exo* directions for NO_2 attack were considered, leading to a total of six transition structures. The computed barrier heights $\Delta H_0^{\ddagger}$ are 136 (eq-*endo*), 139 (eq-*exo*), 141 (aa-*endo*), 142 (ae-*exo*), 146 (ae-*endo*), and 153 (aa-*exo*) kJ/mol. The barrier for *exo* attack on the C_{3v} (all-axial) conformation of RDX has a slightly lower (0.2 mE_h) energy, corresponding to a barrier height of 136 kJ/mol relative to the C_s conformation and 135 kJ/mol relative to the C_{3v} conformer. This structure is listed in Table 2 and illustrated in Figure 2.

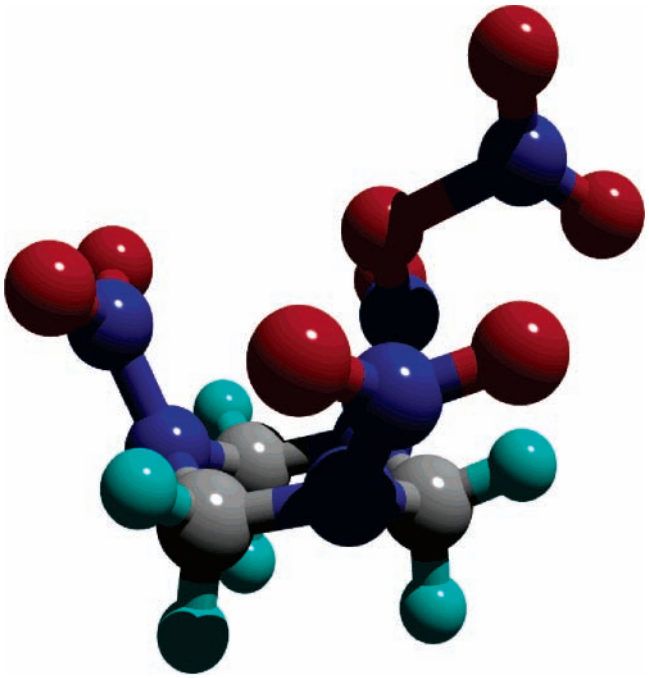

Figure 2. Transition structure for reduction of RDX by NO_2.

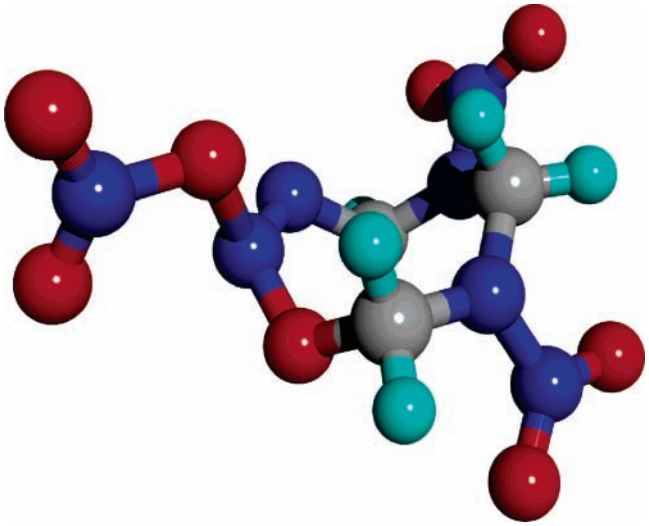

Figure 3. Transition structure for reduction of RDX isomer **1** by NO_2.

The barrier is the same for NO_2 to reduce either H_2NNO_2 or RDX, suggesting that it will be similar for all nitramines. Thus, the barriers for NO_2 to reduce the nitro groups in the products of reactions 1−4 are expected to be about 136 kJ/mol.

For reaction 6, the reactant NO_2 molecules may be spin-coupled as either a singlet (25% probability) or a triplet (75% probability). On the singlet surface, they can approach without a barrier to form $ONONO_2$ ($\Delta H_0 = -8$ kJ/mol). $ONONO_2$ is less stable than its well-known N−N bonded isomer (N_2O_4) by 39 kJ/mol (ΔH_0). In the reverse reaction, singlet-coupled NO and NO_3 also form $ONONO_2$ without a barrier ($\Delta H_0 = -106$ kJ/mol). Thus, reaction 6 has no barrier in excess of its endothermicity when coupled as a spin singlet. On the triplet surface, in contrast, the $^3ONONO_2$ adduct is a transition structure for disproportionation; the barrier is $\Delta H_0^{\ddagger} = 189$ kJ/mol, slightly larger than the barriers for reactions 1 and 4 (see Table 1).

For reaction 7, we started by computing the transition structure for the model reaction $N_2O + NO_2 \rightarrow N_2 + NO_3$. (This yielded $\Delta H_0 = -32$ kJ/mol and the barrier $\Delta H_0^{\ddagger} = 177$ kJ/mol.) Although N_2O and **1** are electronically dissimilar, we hoped that their transition structures would be sufficiently alike to help us locate the transition structure of interest. The important coordinates of this model structure were used to initiate a search for a transition structure for abstraction of an oxygen atom of **1** to yield NO_3 + **2**, reaction 7. This was successful; $\Delta H_0 = 66$ kJ/mol and the barrier $\Delta H_0^{\ddagger} = 139$ kJ/mol for *exo* attack on a conformation with one nitro group axial and one equatorial (ae-*exo*). The transition structure is shown in Figure 3, and its energetics are listed in Table 2. Three higher-lying transition structures were also located: at 144 kJ/mol (ae-*endo*), 144 kJ/mol (aa-*exo*), and 157 kJ/mol (aa-*endo*) relative to **1** + NO_2.

Discussion

Experimental data are available only for reaction 6. Experimental enthalpies of formation at 0 K are 90.8 ± 0.4, 37.0 ± 0.5, and 79.0 ± 1.4 kJ/mol for NO,[22] NO_2,[22] and NO_3,[23] respectively. The corresponding reaction enthalpy is $\Delta H_0 = 96 \pm 2$ kJ/mol, which compares well with our calculated value (97 kJ/mol). Experimentally, reaction 6 has been found to proceed slowly in the gas phase at moderate temperatures.[24]

We assume that secondary reactions are likely to be important early in the reaction only if their energy barriers are comparable to, or smaller than, the barrier for the primary initiation reaction(s). (Later in the reaction the temperature will rise and entropic effects will gain importance, increasing the number of important reactions.) The thermochemistry and barrier heights (Table 1) for initiation reactions 1−4 are compared with those for NO_2 oxidation in Figure 4. Except for triplet-coupled NO_2 disproportionation, the secondary reactions shown have barriers lower than that for any proposed initiation step. Thus, these secondary reactions are likely to be important. We have not considered the effects of entropy or pressure. Since bimolecular reactions are disfavored by entropy ($\Delta S^{\ddagger} < 0$) but favored by pressure ($\Delta V^{\ddagger} < 0$), the net effect will depend upon the reaction conditions.

NO_3 has not been observed in the decomposition, deflagration, or detonation of RDX. However, no effective means of detection has yet been applied. Most contemporary studies involve

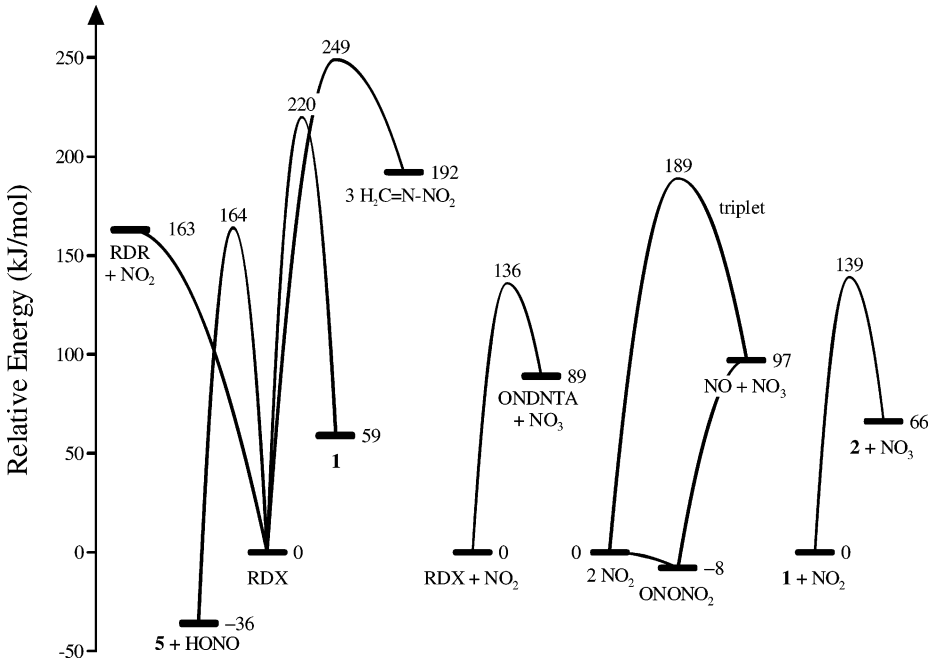

Figure 4. Comparison of energy profiles for initiation and reduction reactions. Energies include ZPE and are at 0 K.

analysis by electron-impact mass spectrometry (EIMS). Unfortunately, EIMS of NO_3 gives little molecular ion; the base peak is NO_2^+.[25] Such a weak signal is likely to be overlooked among the stronger peaks from more abundant species. Another thorough study employed microwave spectroscopy for the analysis,[26] but NO_3 is invisible to that technique because it lacks a permanent dipole moment. Finally, NO_3 is very reactive; even if formed, little might survive subsequent reactions and escape to the gas phase.

An analogous situation was encountered in early investigations of nitramine decomposition.[27] NO_2 was proposed as a prompt product but could not be detected. Failure to detect NO_2 was ascribed to rapid secondary reactions that consumed it.[27,28] Despite the early challenges, NO_2 is now detected routinely and is believed to be a principal primary product.

A more sensitive means of detecting NO_3 (nitrate radical) is needed in nitramine research. Since NO_3 is important in atmospheric chemistry, it has been the subject of excellent reviews.[29,30] One detection method used in that field is laser-induced fluorescence (LIF), for which detection limits as low as 8 parts in 10^{12} by volume (8 pptv) have been reported.[31,32] We encourage experimental investigations of nitramine chemistry using such sensitive analytical methods. If successful, detecting NO_3 vapor may also provide a new means for revealing concealed nitramine explosives.

Acknowledgment. The principal results described herein were presented at the conference "Emerging Methods in Computational Chemistry and Materials Science," in Aberdeen, MD, June 1, 2001. We thank Prof. Peter Politzer and Drs. Marc Nyden, Askar Fahr, and John Merle, and an anonymous referee for helpful comments on the manuscript.

Supporting Information Available: Coordinates, energies (E_e), and unscaled harmonic vibrational frequencies, including infrared intensities, for all minima and saddle points (44 pages). This material is available free of charge via the Internet at http://pubs.acs.org.

References and Notes

(1) Adams, G. F.; Shaw, R. W. *Ann. Rev. Phys. Chem.* **1992**, *43*, 311−340.

(2) Chakraborty, D.; Muller, R. P.; Dasgupta, S.; Goddard, W. A., III. *J. Phys. Chem. A* **2000**, *104*, 2261−2272.

(3) Chakraborty, D.; Muller, R. P.; Dasgupta, S.; Goddard, W. A., III. *J. Phys. Chem. A* **2001**, *105*, 1302−1314.

(4) Irikura, K. K.; Johnson, R. D., III. *J. Phys. Chem. A* **2000**, *104*, 2191−2194.

(5) Stewart, J. J. P. *J. Comput. Chem.* **1989**, *10*, 209−220.

(6) Melius, C. F. In *Chemistry and Physics of Energetic Materials*; Bulusu, S. N., Ed.; Kluwer Academic: Dordrecht, 1990; pp 21−49.

(7) Behrens, R., Jr.; Bulusu, S. *J. Phys. Chem.* **1992**, *96*, 8891−8897.

(8) Certain commercial materials and equipment are identified in this paper in order to specify procedures completely. In no case does such identification imply recommendation or endorsement by the National Institute of Standards and Technology, nor does it imply that the material or equipment identified is necessarily the best available for the purpose.

(9) Frisch, M. J.; Trucks, G. W.; Schlegel, H. B.; Scuseria, G. E.; Robb, M. A.; Cheeseman, J. R.; Zakrzewski, V. G.; Montgomery, J. A., Jr.; Stratmann, R. E.; Burant, J. C.; Dapprich, S.; Millam, J. M.; Daniels, A. D.; Kudin, K. N.; Strain, M. C.; Farkas, O.; Tomasi, J.; Barone, V.; Cossi, M.; Cammi, R.; Mennucci, B.; Pomelli, C.; Adamo, C.; Clifford, S.; Ochterski, J.; Petersson, G. A.; Ayala, P. Y.; Cui, Q.; Morokuma, K.; Malick, D. K.; Rabuck, A. D.; Raghavachari, K.; Foresman, J. B.; Cioslowski, J.; Ortiz, J. V.; Stefanov, B. B.; Liu, G.; Liashenko, A.; Piskorz, P.; Komaromi, I.; Gomperts, R.; Martin, R. L.; Fox, D. J.; Keith, T.; Al-Laham, M. A.; Peng, C. Y.; Nanayakkara, A.; Gonzalez, C.; Challacombe, M.; Gill, P. M. W.; Johnson, B.; Chen, W.; Wong, M. W.; Andres, J. L.; Gonzalez, C.; Head-Gordon, M.; Replogle, E. S.; Pople, J. A. *Gaussian 98*, revision A.7; Gaussian, Inc.: Pittsburgh, PA, 1998.

(10) Schmidt, M. W.; Baldridge, K. K.; Boatz, J. A.; Jensen, J. H.; Koseki, S.; Gordon, M. S.; Nguyen, K. A.; Windus, T. L.; Elbert, S. T. *QCPE Bull.* **1990**, *10*, 52−54.

(11) Schmidt, M. W.; Baldridge, K. K.; Boatz, J. A.; Elbert, S. T.; Gordon, M. S.; Jensen, J. H.; Koseki, S.; Matsunaga, N.; Nguyen, K. A.; Su, S. J.; Windus, T. L.; Dupuis, M.; Montgomery, J. A. *J. Comput. Chem.* **1993**, *14*, 1347−1363.

(12) Granovsky, A. A. *PC-GAMESS*, revision 6.0; Moscow State University: Moscow, 2000.

(13) Becke, A. D. *J. Chem. Phys.* **1993**, *98*, 5648−5652.

(14) Stephens, P. J.; Devlin, F. J.; Chabalowski, C. F.; Frisch, M. J. *J. Phys. Chem.* **1994**, *98*, 11623−11627.

(15) Lee, C.; Yang, W.; Parr, R. G. *Phys. Rev. B* **1988**, *37*, 785−789.

(16) Frisch, M. J.; Trucks, G. W.; Schlegel, H. B.; Scuseria, G. E.; Robb, M. A.; Cheeseman, J. R.; Montgomery, J. A., Jr.; Vreven, T.; Kudin, K. N.; Burant, J. C.; Millam, J. M.; Iyengar, S. S.; Tomasi, J.; Barone, V.; Mennucci, B.; Cossi, M.; Scalmani, G.; Rega, N.; Petersson, G. A.; Nakatsuji, H.; Hada, M.; Ehara, M.; Toyota, K.; Fukuda, R.; Hasegawa, J.; Ishida, M.; Nakajima, T.; Honda, Y.; Kitao, O.; Nakai, H.; Klene, M.; Li, X.; Knox, J. E.; Hratchian, H. P.; Cross, J. B.; Adamo, C.; Jaramillo, J.; Gomperts, R.; Stratmann, R. E.; Yazyev, O.; Austin, A. J.; Cammi, R.; Pomelli, C.; Ochterski, J. W.; Ayala, P. Y.; Morokuma, K.; Voth, G. A.; Salvador, P.; Dannenberg, J. J.; Zakrzewski, V. G.; Dapprich, S.; Daniels, A. D.; Strain, M. C.; Farkas, O.; Malick, D. K.; Rabuck, A. D.; Raghavachari, K.; Foresman, J. B.; Ortiz, J. V.; Cui, Q.; Baboul, A. G.; Clifford, S.; Cioslowski, J.; Stefanov, B. B.; Liu, G.; Liashenko, A.; Piskorz, P.; Komaromi, I.; Martin, R. L.; Fox, D. J.; Keith, T.; Al-Laham, M. A.; Peng, C. Y.; Nanayakkara, A.; Challacombe, M.; Gill, P. M. W.; Johnson, B.; Chen, W.; Wong, M. W.; Gonzalez, C.; Pople, J. A. *Gaussian 03*, revision B.05; Gaussian, Inc.: Pittsburgh, PA, 2003.

(17) Gonzalez, C.; Schlegel, H. B. *J. Phys. Chem.* **1990**, *94*, 5523−5527.

(18) Scott, A. P.; Radom, L. *J. Phys. Chem.* **1996**, *100*, 16502−16513.

(19) Johnson, R. D., III. *NIST Computational Chemistry Comparison and Benchmark Database*, version 12; NIST Standard Reference Database Number 101; August 2005; National Institute of Standards and Technology: http://srdata.nist.gov/cccbdb/.

(20) Irikura, K. K.; Johnson, R. D., III; Kacker, R. N. *Metrologia* **2004**, *41*, 369−375.

(21) Harris, N. J.; Lammertsma, K. *J. Am. Chem. Soc.* **1997**, *119*, 6583−6589.

(22) *Thermodynamic Properties of Individual Substances*, 4th ed.; Gurvich, L. V., Veyts, I. V., Alcock, C. B., Eds.; Hemisphere: New York, 1989.

(23) Davis, H. F.; Kim, B. S.; Johnston, H. S.; Lee, Y. T. *J. Phys. Chem.* **1993**, *97*, 2172−2180.

(24) *Chemical Kinetics Database (Standard Reference Database 17)*, version 7.0 (web version), release 1.3; National Institute of Standards and Technology: http://kinetics.nist.gov/.

(25) Seisel, S.; Caloz, F.; Fenter, F. F.; van den Bergh, H.; Rossi, M. J. *Geophys. Res. Lett.* **1997**, *24*, 2757−2760.

(26) Lovas, F. J.; Suenram, R. D. *Thermal Decomposition Pathways in Nitramine Propellants*, USARO Contract No. 29596-CH. Physics Laboratory, Molecular Physics Division, National Institute of Standards and Technology, 1995.

(27) Flournoy, J. M. *J. Chem. Phys.* **1962**, *36*, 1106−1107.

(28) Schroeder, M. A. Critical Analysis of Nitramine Decomposition Data Product Distributions from HMX and RDX Decomposition. *Proceedings of the 18th JANNAF Combustion Meeting*, Pasadena, California, 1981; pp 395−413.

(29) Atkinson, R. *J. Phys. Chem. Ref. Data* **1991**, *20*, 459−507.

(30) Wayne, R. P.; Barnes, I.; Biggs, P.; Burrows, J. P.; Canosa-Mas, C. E.; Hjorth, J.; Le Bras, G.; Moortgat, G. K.; Perner, D.; Poulet, G.; Restelli, G.; Sidebottom, H. *Atmos. Environ.* **1991**, *25A*, 1−203.

(31) Wood, E. C.; Wooldridge, P. J.; Freese, J. H.; Albrecht, T.; Cohen, R. C. *Environ. Sci. Technol.* **2003**, *37*, 5732−5738.

(32) Matsumoto, J.; Imai, H.; Kosugi, N.; Kaji, Y. *Atmos. Environ.* **2005**, *39*, 6802−6811.

(33) Rauch, F. C.; Fanelli, A. J. *J. Phys. Chem.* **1969**, *73*, 1604−1608.

(34) Robertson, A. J. B. *Trans. Faraday Soc.* **1949**, *45*, 85−93.

(35) Zhao, X.; Hintsa, E. J.; Lee, Y. T. *J. Chem. Phys.* **1988**, *88*, 801−810.

(36) Bradley, J. N.; Butler, A. K.; Capey, W. D.; Gilbert, J. R. *J. Chem. Soc., Faraday Trans. I* **1977**, *73*, 1789−1795.